

ADVANCED FUNCTIONAL MATERIALS

Supporting Information

for *Adv. Funct. Mater.*, DOI: 10.1002/adfm.202101175

Tuning the Photophysical and Electrochemical
Properties of Aza-Boron-Dipyridylmethenes for
Fluorescent Blue OLEDs

*Abegail C. Tadle, Karim A. El Roz, Chan Ho Soh, Daniel
Sylvinson Muthiah Ravinson, Peter I. Djurovich, Stephen
R. Forrest, and Mark E. Thompson**

Supporting Information

Tuning the Photophysical and Electrochemical Properties of Aza-boron-dipyridylmethene for Fluorescent Blue OLEDs

Abigail C. Tadle,¹ Karim A. El Roz,¹ Chan Ho Soh,² Daniel Sylvinson Muthiah Ravinson,¹ Peter I. Djurovich,¹ Stephen R. Forrest,^{2,3,4} Mark E. Thompson^{1,5,}*

¹ Department of Chemistry, University of Southern California, Los Angeles, California, 90089, USA

² Department of Physics, University of Michigan, Ann Arbor, Michigan 48109, USA · ³ Department of Electrical and Computer Engineering, University of Michigan, Ann Arbor, Michigan 48109, USA

⁴ Department of Materials Science and Engineering, University of Michigan, Ann Arbor, Michigan 48109, USA

⁵ Mork Family Department of Chemical Engineering and Materials Science, University of Southern California, Los Angeles, California, 90089, USA

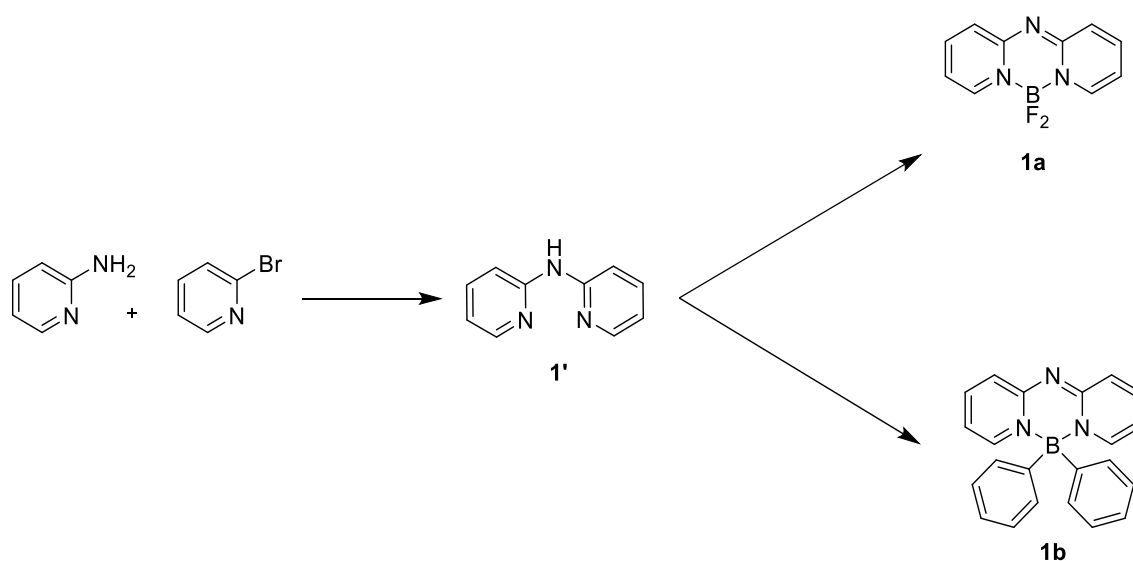
* To whom correspondence should be addressed. Email: met@usc.edu

Contents

Synthesis	3
difluoro-boron complex of 2,2'-dipyridylamine (1a):	4
diphenyl-boron complex of 2,2'-dipyridylamine (1b):.....	4
difluoro-boron complex of 2,2'-diquinolylamine (2a):	5
difluoro-boron complex of bis(6-isopropylquinoline-2-yl)amine (2b):	8
difluoro-boron complex of 5-methoxy-N-(quinolin-2-yl)quinolin-2-amine) (2c):.....	9
difluoro-boron complex of 2,2'-di-5-methoxyquinolylamine (2d):.....	11
difluoro-boron complex of 2,2'-diisoquinolylamine (3):	11
difluoro-boron complex of N-(isoquinolin-1-yl)-5-methoxyquinolin-2-amine) (4):	12
Photophysical Characterization	13
Table S1. Calculated and Experimental S1 and T1 energies for 1a-1b, 2a-2d, 3 and 4, where the difference between the two energies are represented by $\Delta E(S_1-T_1)$	13
Table S2. Summary of the photophysical parameters for 1a-1b, 2a-2d, 3 and 4.	14
Figure S1. Normalized Spectra of absorbance (dash), fluorescence (solid) at 298K, and phosphorescence emission at 77K in 2-MeTHF for 1a and 1b.....	14
Figure S2. Normalized Spectra of absorbance (dash), fluorescence (solid) at 298K, and phosphorescence emission at 77K in 2-MeTHF for 2a, 2b, 2c, 2d, 3 and 4	15
Figure S3. Normalized absorbance and emission of 2a in three different solvents.....	16
Electrochemistry	17
Table S3. HOMO and LUMO energies (in eV) for 1a-1b, 2a-2d, 3 and 4	17
Figure S4. Cyclic Voltammetry for the compounds in acetonitrile vs ferrocene (100 mV/s).	18
TDDFT Calculations	19
Table S4. Extent of overlap calculation using TDDFT with experimental comparison.....	20
Table S5. Calculated excited state energies (in eV) at S_0 and S_1 optimized geometries. (B3LYP/6-311G**) for 2a-2d, 3 and 4	20
Table S6. Molecular orbital representation of compounds 1a-1b, 2a-2d, 3 and 4 at the B3LYP/6-311G** level.	21
Organic LEDs	22
Figure S5. Photoluminescence data for doped and neat 2a films, which shows a decrease in the emission peak around 450 nm of 2a due to reabsorption as concentration increases.....	23
Figure S6. OLED data for 1% 2a doped film with CBP as host.....	24
Figure S7. OLED data for 1% 2a doped film with 26DCzPPY as host.....	25
Figure S8. OLED data for 1% 2a doped film with DPEPO as host.....	26
Thermogravimetric Analysis of azaDIPYR, α-azaDIPYR and α-DIPYR	27
Figure S9. Thermogravimetric analysis curves for azaDIPYR (1a), α -azaDIPYR (2a) and α -DIPYR.	27

Synthesis

Synthesis of the reported materials follow a similar previously reported procedure.¹ The synthetic route for aD dyes follows a palladium catalyzed coupling reaction of 2-amino and 2-bromo substituted quinoline core to form the desired ligand. 2-chloro substituted quinoline core can be used in place of the latter. After purification of the ligand, it was deprotonated with Hunig's base and chelation of the ligand with boron difluorides was accomplished by refluxing with trifluoride diethyl etherate. The purified products produced a white powder for the non-benzannulated aD compounds (**1a-1b**) and a yellow powder for the benzannulated aD compounds (**2a-2d**, **3** and **4**). Discussion of **2d** in the paper is omitted because we are unable to get satisfactory CHNS data. However, all data collected for **2d** are included in the SI.



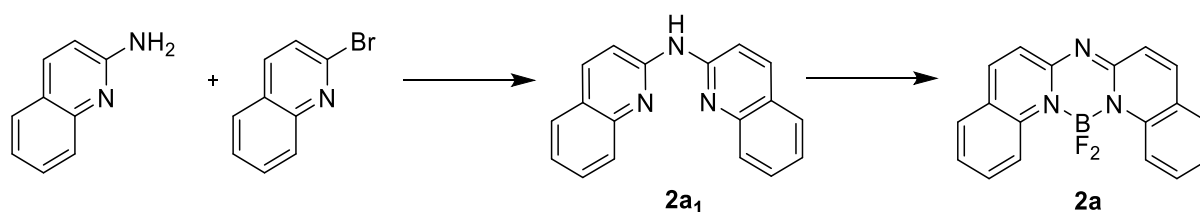
Scheme S1. Synthesis of **1a** and **1b**.

2,2'-dipyridylamine (**1'**): bis(2-diphenylphosphinophenyl) ether(498.99mg, 926.51 μ mol), 2-bromopyridine(3.66, 23.16mmol), 2-aminopyridine (2.18g, 23.16mmol) and t-BuONa (3.12g, 32.43mmol) were purged with nitrogen gas in a re-sealable shlenk flask where a degassed dry toluene is cannula transferred. Pd(OAc)₂ catalyst was added to the air free flask and refluxed in a 110 °C oil bath for 24 hours. The reaction mixture is cooled to room temperature and diluted with THF and ethyl ether. The solid precipitate was filtered, concentrated, and purified via silica gel column chromatography (2% MeOH/CH₂Cl₂). An alternative route is to purchase the commercially available

2,2'-dipyridylamine. $^1\text{H NMR}$ (400 MHz, $\text{DMSO-}d_6$) δ 9.61 (s, 1H), 8.19 (ddd, $J = 4.9, 2.0, 0.9$ Hz, 1H), 7.71 (dt, $J = 8.4, 1.0$ Hz, 1H), 7.65 – 7.59 (m, 1H), 6.84 (ddd, $J = 7.1, 4.9, 1.1$ Hz, 1H).

difluoro-boron complex of 2,2'-dipyridylamine (1a): A solution of the 2,2'-dipyridylamine ligand (300mg, 1.75mmol) in dry 1,2-dichloroethane was prepared in an N_2 -purged schlenk flask equipped with a magnetic stir bar and fitted with a reflux condenser. The flask was submerged in a preheated oil bath and brought to reflux, at which time 2.0 eq. boron trifluoride diethyl etherate (497.40mg, 3.50mmol) were added dropwise. The solution was stirred for 2 hours at reflux, then cooled to room temperature and treated with 5 eq. N,N -diisopropylethylamine (1.53mL, 8.70mmol). The solution was washed with water and the aqueous layer was separated and extracted three times with dichloromethane. The organic layers were combined, dried over sodium sulfate, filtered, and reduced concentrated by rotary evaporation. The products were purified by silica gel flash chromatography with the eluent 50% dichloromethane in hexanes. $^1\text{H NMR}$ (400 MHz, $\text{DMSO-}d_6$) δ 8.06 (dd, $J = 5.6, 3.2$ Hz, 1H), 7.86 (dddd, $J = 8.7, 6.8, 1.8, 0.4$ Hz, 1H), 7.14 (d, $J = 8.8$ Hz, 1H), 7.01 (td, $J = 6.7, 1.3$ Hz, 1H). $^{13}\text{C NMR}$ (101 MHz, $\text{DMSO-}d_6$) δ 141.48, 136.65, 122.47, 114.95 (d, $J = 2.6$ Hz). Elemental Analysis: calc. (C, 54.84; H, 3.68; N, 19.19), found (C, 54.74; H, 3.86; N, 18.76)

diphenyl-boron complex of 2,2'-dipyridylamine (1b): A solution of the 2,2'-dipyridylamine ligand (800mg, 4.67mmol) and 2-aminoethoxydiphenylborate (1.05g, 4.67mmol) in dry 1,2-dichloroethane was prepared in an N_2 -purged schlenk flask equipped with a magnetic stir bar and fitted with a reflux condenser. The flask was submerged in a preheated oil bath and brought to reflux for 16 hours. The solution was washed with water and the aqueous layer was separated and extracted three times with dichloromethane. The organic layers were combined, dried over sodium sulfate, filtered, and reduced concentrated by rotary evaporation. The product was purified by silica gel flash chromatography with 100% ethylacetate then 100% acetone. $^1\text{H NMR}$ (400 MHz, acetone- d_6) δ 7.96 (dd, $J = 6.4, 1.9, 0.9$ Hz, 1H), 7.87 (dt, $J = 7.9, 1.2$ Hz, 4H), 7.63 (dddd, $J = 8.6, 6.8, 1.8, 0.9$ Hz, 1H), 7.41 (tt, $J = 6.3, 1.4$ Hz, 2H), 7.41 – 7.30 (m, 4H), 7.22 (d, $J = 7.3$ Hz, 1H), 7.18 – 7.03 (m, 3H), 6.97 – 6.90 (m, 1H), 6.78 – 6.70 (m, 1H).



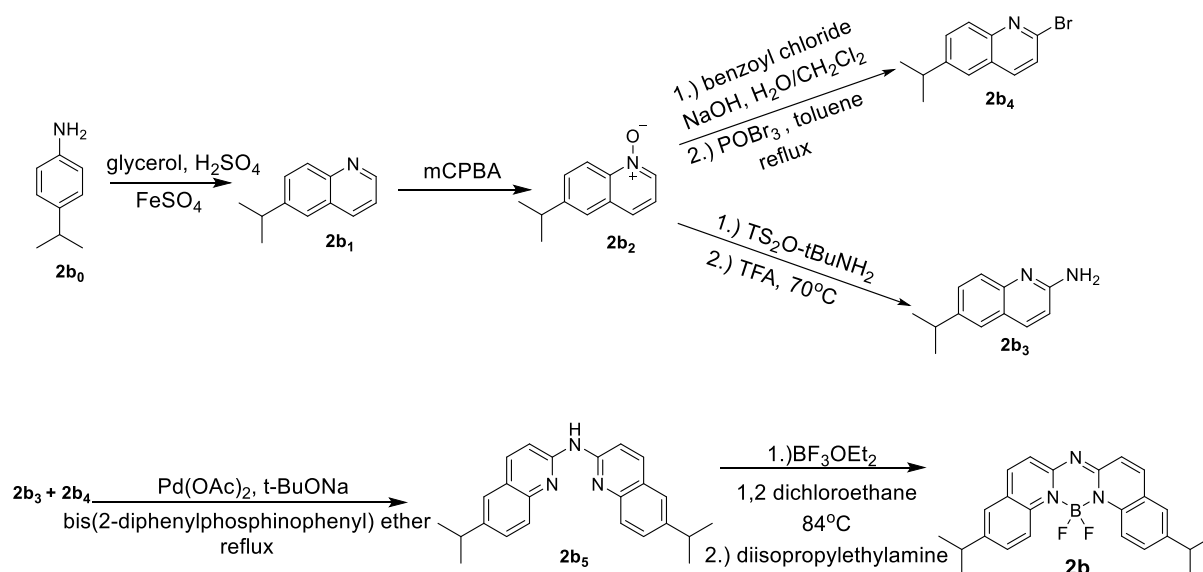
Scheme S2. Synthesis of **2a**.

2,2'-diquinolyamine (2a₁): bis(2-diphenylphosphinophenyl) ether (395.03 mg, 733.48 μmol), 2-bromoquinoline (3.00 g, 18.34 mmol), 2-aminoquinoline (2.78 g, 19.25 mmol) and t-BuONa (2.47 g, 25.67 mmol) were purged with nitrogen gas in a re-sealable shlenk flask where degassed dry toluene is cannula transferred. Pd(OAc)₂ (164.67, 733.48 μmol) catalyst was added to the air free flask and refluxed in a 110°C oil bath for 24 hours. The reaction mixture is cooled to room temperature and diluted with THF and ethylether. The solid precipitate was filtered, concentrated, and purified via silica gel column chromatography (2% MeOH/CH₂Cl₂). A white solid is isolated upon purification (40-80% yield). ¹H NMR (400 MHz, DMSO-*d*₆) δ 10.43 (s, 1H), 8.33 – 8.17 (m, 4H), 7.83 (ddd, *J* = 8.1, 1.5, 0.6 Hz, 2H), 7.77 (ddt, *J* = 8.4, 1.2, 0.6 Hz, 2H), 7.64 (ddd, *J* = 8.4, 6.9, 1.5 Hz, 2H), 7.38 (ddd, *J* = 8.0, 6.9, 1.2 Hz, 2H).

difluoro-boron complex of 2,2'-diquinolyamine (2a): A 15 mM solution of 2,2'-diquinolyamine in dry 1,2-dichloroethane was prepared in an N₂-purged schlenk flask equipped with a magnetic stir bar and fitted with a reflux condenser. The flask was submerged in a preheated oil bath and brought to reflux, at which time 2.0 eq. boron trifluoride diethyletherate were added dropwise. The solution was stirred for 2 hours at reflux, then cooled to room temperature and treated with 5 eq. N,N-diisopropylethylamine, causing the precipitate to dissolve. The solution was washed with water and the aqueous layer was separated and extracted three times with dichloromethane. The organic layers were combined, dried over sodium sulfate, filtered, and reduced concentrated by rotary evaporation. The products were purified by silica gel flash chromatography with the eluent 2% MeOH/CH₂Cl₂ solvent mixture in hexanes. For further purification, the material was sublimed at ~200 °C at 1.6x10⁻⁶ Torr. ¹H NMR (400 MHz, DMSO-*d*₆) δ 8.46 – 8.39 (m, 1H), 8.39 – 8.32 (m, 1H), 7.94 (dd, *J* = 7.9, 1.6 Hz, 1H), 7.79 (ddd, *J* = 8.8, 7.1, 1.6 Hz, 1H), 7.53 (ddd, *J* = 7.9, 7.1, 0.9 Hz, 1H), 7.25 (d, *J* = 9.0

Hz, 1H). ^{13}C NMR (101 MHz, $\text{DMSO}-d_6$) δ 154.10, 141.98, 131.71, 129.43, 125.73, 122.98.

Elemental Analysis: calc. (C, 67.75; H, 3.79; N, 13.17), found (C, 67.40; H, 3.81; N, 12.70)



Scheme S3. Synthesis of **2b**.

6-isopropylquinoline (**2b**₁): 4-isopropylaniline (**2b**₀) (20 g, 0.147 moles), nitrobenzene (9.86 ml, 0.096 moles), Glycerol (55.85 g, 0.606 moles), and $\text{FeSO}_4 \cdot 7\text{H}_2\text{O}$ (5.14 g, 18.49 moles) were added to a three-neck round bottom flask. While the flask was kept in an ice bath, H_2SO_4 (25 ml, 0.473 moles) was added slowly to the reaction mixture. After the addition was completed, the ice bath was removed followed by refluxing the mixture for 20 h under inert conditions. After cooling to room temperature, the pH of the solution was adjusted to pH 7 with 50 % NaOH aq. Then, solution was extracted with diethyl ether. After the extraction, MgSO_4 was used as a drying agent. Filtration followed by evaporation to give a brown liquid. The product was isolated by reduced pressure distillation to yield the desired light-yellow liquid (yield 20 %). ^1H NMR (400 MHz, CDCl_3) δ 8.85 (dd, $J = 4.2, 1.7$ Hz, 1H), 8.10 (dddd, $J = 8.3, 1.7, 0.9, 0.4$ Hz, 1H), 8.04 (dt, $J = 8.6, 0.8$ Hz, 1H), 7.65 – 7.59 (m, 2H), 7.36 (dd, $J = 8.2, 4.2$ Hz, 1H), 3.10 (hept, $J = 6.9$ Hz, 1H), 1.38 – 1.33 (m, 8H).

6-isopropylquinoline-1-oxide (**2b**₂): Compound (**2b**₁) (10.2 g, 0.059 moles) was dissolved in one-neck round bottom flask with CH_2Cl_2 (50 ml). *m*-chloroperoxybenzoic acid (mCPBA) (12.33 g, 0.071 moles) was added slowly the stirred solution at room temperature. The reaction was stirred overnight.

Next, saturated NaHCO_3 aq solution was added to stirring solution until no CO_2 gas bubbles were observed anymore. Then, pH was adjusted to 10 with NaOH aq solution and extracted with CH_2Cl_2 50 ml three times. The solution was dried over MgSO_4 . The solvent was removed under reduced pressure. The crude product was then purified by silica gel column chromatography (2 % methanol/ CH_2Cl_2). White pale-yellow solid was afforded at 60 % yield. $^1\text{H NMR}$ (400 MHz, CDCl_3) δ 8.66 (dd, $J = 8.8, 0.8$ Hz, 1H), 8.47 (dd, $J = 6.0, 1.0$ Hz, 1H), 7.71 – 7.63 (m, 3H), 7.26 – 7.23 (m, 1H), 3.10 (hept, $J = 6.9$ Hz, 1H), 1.34 (dd, $J = 6.9, 0.5$ Hz, 6H).

6-isopropylquinoline-2-amine ($2b_3$): To a round bottom flask, compound ($2b_2$) (2.55 g, 0.013 moles) and 30 ml of trifluorotoluene (7.16 ml, 0.068 moles) were mixed in 20 ml of chloroform. After compound ($2b_2$) was dissolved, the mixture was cooled to 0 °C with an ice bath. T-butylamine (7.16 ml, 0.068 moles) was added slowly followed by Ts_2O (8.89 g, 0.027 moles). The reaction was left to stir for two hours. If the reaction were not completed, portions of t-butylamine (0.6 equiv. to 4.0 equiv.) and Ts_2O (0.3 equiv. to 2.3 equiv.) would be added until the reaction is completed. The reaction was then treated with 25 ml TFA at 70 °C for overnight under inert atmosphere. After that, most of the solvents were removed under reduced pressure and then the concentrated oil residue was diluted with CH_2Cl_2 and quenched with 50 % of aq solution of NaOH to pH 10. The solution was extracted with CH_2Cl_2 three times, dried over MgSO_4 , and removed under reduced pressure. The crude product was then purified using a silica gel column chromatography (2% methanol/ CH_2Cl_2). The desired white solid was obtained at 70 %. $^1\text{H NMR}$ (400 MHz, CDCl_3) δ 7.92 (dd, $J = 9.0, 0.8$ Hz, 1H), 7.70 – 7.64 (m, 1H), 7.52 (dd, $J = 8.7, 2.0$ Hz, 1H), 7.46 (d, $J = 2.0$ Hz, 1H), 6.80 (d, $J = 9.0$ Hz, 1H), 6.29 (s, 2H), 3.02 (hept, $J = 6.9$ Hz, 1H), 1.30 (dd, $J = 6.9, 0.9$ Hz, 6H).

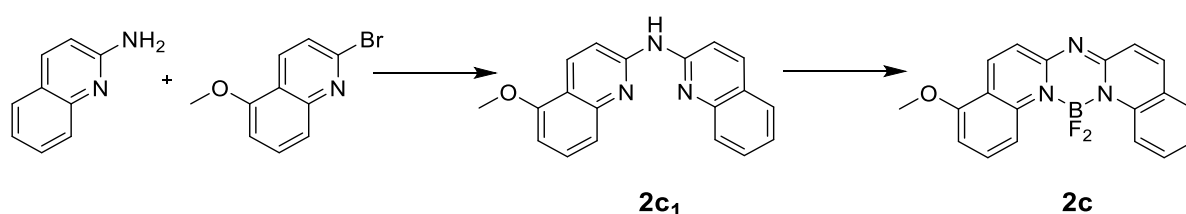
2-bromo-6-isopropylquinoline ($2b_4$): To a round bottom flask cooled to 5 °C with an ice bath, benzoyl chloride (2.33 ml, 0.02 mol) was added slowly to the vigorously stirred mixture of compound ($2b_2$) (2.5 g, 0.0133 mol), sodium hydroxide (1 g, 0.025 mol) in water (12 ml) and CH_2Cl_2 (10 ml). After the addition is complete, the reaction mixture was left to stir for few hours. Then, the mixture was extracted from CH_2Cl_2 . The combined organic layer was dried over MgSO_4 . Solvent was removed

under reduced pressure to obtain a white solid product. After that, the solid was mixed with POBr_3 (2.2 g, 0.007 mol) in dry toluene (20 ml) under inert atmosphere, heated to reflux overnight. After cooling to room temperature, the mixture was poured on ice, washed with saturated NaHCO_3 and extracted with CH_2Cl_2 several times. The solvent was removed under reduced pressure. The crude product was then purified using a silica gel column chromatography (50 % hexane/ CH_2Cl_2). The desired white solid was obtained at 40 %. $^1\text{H NMR}$ (400 MHz, CDCl_3) δ 8.20 – 8.13 (m, 1H), 7.99 – 7.92 (m, 2H), 7.71 – 7.61 (m, 1H), 7.57 – 7.50 (m, 1H), 3.09 (hept, $J = 6.9$ Hz, 1H), 1.34 (dd, $J = 6.8$, 0.5 Hz, 6H).

Bis(6-isopropylquinoline-2-yl)amine ($2b_5$): Compound ($2b_3$) (2.23 g, 0.012 mol) and compound ($2b_4$) (3 g, 0.012 mol) were mixed with bis(2-diphenylphosphinophenyl)ether (0.246 g, 4 % mmol), *t*-BuONa (1.54 g, 0.016 mol), and $\text{Pd}(\text{OAc})_2$ (0.1 g, 4 % mmol) in a three-neck round bottom flask. The flask was subjected to three cycles of evacuation-backfilling with N_2 . Dry toluene purged with N_2 was transferred to the reaction mixture using a cannula. The reaction was refluxed for 48 h at 110 °C under inert atmosphere. After that, the mixture was cooled to room temperature, extracted from CH_2Cl_2 , dried over MgSO_4 , and solvent removed under reduced pressure. The crude product was then purified using a silica gel column chromatography (2% methanol/ CH_2Cl_2). The desired white solid was obtained at 50 %. $^1\text{H NMR}$ (400 MHz, CDCl_3) δ 8.05 (d, $J = 8.9$ Hz, 1H), 7.98 (dd, $J = 11.2$, 8.8 Hz, 1H), 7.79 (d, $J = 8.6$ Hz, 1H), 7.73 (d, $J = 8.6$ Hz, 1H), 7.59 – 7.48 (m, 2H), 3.07 (pd, $J = 6.9$, 2.5 Hz, 1H), 1.35 (ddd, $J = 6.9$, 1.6, 0.5 Hz, 6H).

difluoro-boron complex of bis(6-isopropylquinoline-2-yl)amine ($2b$): Compound ($2b_5$) (1 g, 0.0028 mol) was dissolved in dry toluene under N_2 in a three-neck round bottom flask. DIEA (1.47 ml, 0.008 mol) was slowly injected to the solution. After 30 min stirring, BF_3OEt_2 (1.39 ml, 0.0011 mol) was slowly added dropwise to the solution. The reaction was then left to reflux overnight. After cooling to room temperature, saturated solution of NaHCO_3 aq was added to the reaction mixture, followed by extraction from CH_2Cl_2 . The combined organic layers were dried over MgSO_4 , and solvent removed under reduced pressure. The crude product was purified by silica gel

chromatography (50 % hexane/ethyl acetate) to afford a yellow solid. The desired product was further sublimed at 190 °C under 1.2×10^{-6} torr. $^1\text{H NMR}$ (400 MHz, CDCl_3) δ 8.57 (dt, $J = 8.9, 3.4$ Hz, 1H), 7.99 – 7.94 (m, 1H), 7.62 (dd, $J = 9.0, 2.2$ Hz, 1H), 7.50 (d, $J = 2.2$ Hz, 1H), 7.17 (d, $J = 9.0$ Hz, 1H), 3.06 (hept, $J = 6.9$ Hz, 1H), 1.34 (d, $J = 7.0$ Hz, 6H). $^{13}\text{C NMR}$ (101 MHz, $\text{DMSO}-d_6$) δ 153.68, 145.85, 141.72, 130.78, 125.97, 124.89, 122.82, 121.34, 33.30, 24.12. Elemental Analysis: calc. (C, 71.48; H, 6.00; N, 10.42), found (C, 71.38; H, 5.94; N, 10.36)

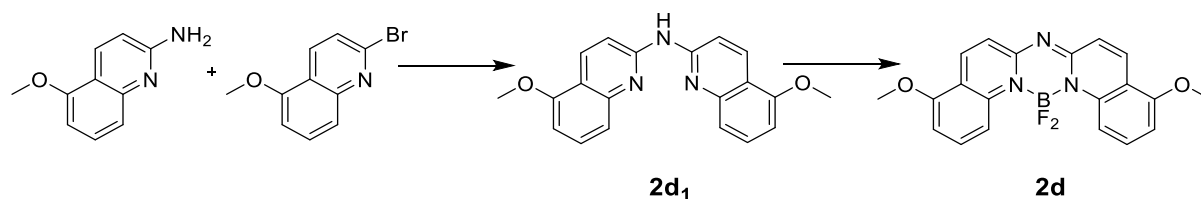


Scheme S4: Synthesis of **2c**.

5-methoxy-*N*-(quinolin-2-yl)quinolin-2-amine (**2c₁**): bis(2-diphenylphosphinophenyl) ether (17.23 mg, 32 μmol), 2-bromo-5-methoxyquinoline (200 mg, 0.84 mmol), 2-aminoquinoline (121 mg, 0.84 mmol) and *t*-BuONa (107.64 mg, 1.12 mmol), and $\text{Pd}(\text{OAc})_2$ (7.18 mg, 32 μmol) catalyst were added to a three-neck round bottom flask. The air free flask and refluxed in a 110 °C oil bath for 48 hours. The flask was subjected to three cycles of evacuation-backfilling with N_2 . Dry toluene purged with N_2 was transferred to the reaction mixture using a cannula. The reaction was refluxed for 48 h at 110 °C under inert atmosphere. After that, the mixture was cooled to room temperature, extracted from CH_2Cl_2 , dried over MgSO_4 , and solvent removed under reduced pressure. The crude product was then purified using a silica gel column chromatography (2% methanol/ CH_2Cl_2). $^1\text{H NMR}$ (400 MHz, CDCl_3) δ 7.93 – 7.84 (m, 2H), 7.71 – 7.60 (m, 4H), 7.56 (ddd, $J = 8.4, 6.9, 1.5$ Hz, 1H), 7.40 – 7.35 (m, 2H), 7.23 – 7.19 (m, 1H), 7.19 – 7.15 (m, 1H), 3.94 (s, 3H).

difluoro-boron complex of 5-methoxy-*N*-(quinolin-2-yl)quinolin-2-amine (**2c**): In a three-neck round bottom flask, the ligand, 5-methoxy-*N*-(quinolin-2-yl)quinolin-2-amine (**2c₁**) (500 mg, 1.51 mmol) was dissolved in dry toluene under N_2 . DIEA (0.79 ml, 4.53 mmol) was slowly injected to the

solution. After 30 min of stirring, BF_3OEt_2 (0.745 ml, 6.04 mmol) was slowly added dropwise to the solution. The reaction was then left to reflux overnight. After cooling to room temperature, saturated solution of NaHCO_3 aq was added to the reaction mixture, followed by extraction from CH_2Cl_2 . The combined organic layers were dried over MgSO_4 , and solvent removed under reduced pressure. The crude product was purified by silica gel chromatography (2% methanol/ CH_2Cl_2) to afford a yellow solid. The desired product was further sublimed at $200\text{ }^\circ\text{C}$ under 1.2×10^{-6} torr. ^1H NMR (400 MHz, $\text{DMSO-}d_6$) δ 9.19 – 9.11 (m, 2H), 7.98 – 7.89 (m, 6H), 7.86 – 7.75 (m, 2H), 7.48 (dt, $J = 7.0, 1.0$ Hz, 2H), 1.20 (s, 1H). ^{13}C NMR (101 MHz, dms) δ 152.56, 136.90, 134.04, 129.61, 129.03, 127.88, 127.12, 114.80, 40.59, 40.39, 40.18, 39.97, 39.76, 39.55, 39.34. Elemental Analysis: calc. (C, 65.36; H, 4.04; N, 12.04), found (C, 65.42; H, 4.33; N, 11.47)

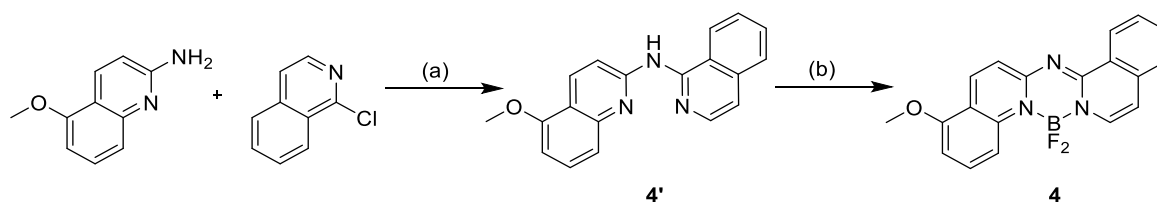


Scheme S5. Synthesis of **2d**.

2,2'-di-5-methoxyquinolyamine ($2d_1$): bis(2-diphenylphosphinophenyl) ether (43 mg, 80 μmol), 2-bromo-5-methoxyquinoline (500 mg, 2.1 mmol), 2-amino-5-methoxyquinoline (365 mg, 2.1 mmol) and *t*-BuONa (269 mg, 2.8 mmol), and $\text{Pd}(\text{OAc})_2$ (17.96 mg, 80 μmol) catalyst were added to a three-neck round bottom flask. The air free flask and refluxed in a $110\text{ }^\circ\text{C}$ oil bath for 48 hours. The flask was subjected to three cycles of evacuation-backfilling with N_2 . Dry toluene purged with N_2 was transferred to the reaction mixture using a cannula. The reaction was refluxed for 48 h at $110\text{ }^\circ\text{C}$ under inert atmosphere. After that, the mixture was cooled to room temperature, extracted from CH_2Cl_2 , dried over MgSO_4 , and solvent removed under reduced pressure. The crude product was then purified using a silica gel column chromatography (2% methanol/ CH_2Cl_2). ^1H NMR (400 MHz, CDCl_3) δ 8.01 (d, $J = 8.8$ Hz, 1H), 7.89 (s, 1H), 7.83 (d, $J = 8.8$ Hz, 1H), 7.61 (d, $J = 8.8$ Hz, 1H), 7.28 – 7.19 (m, 1H), 7.03 (ddd, $J = 8.8, 2.5, 0.5$ Hz, 1H), 5.30 (d, $J = 0.5$ Hz, 1H), 3.95 (s, 3H). ^{13}C NMR (101 MHz, $\text{DMSO-}d_6$) δ 161.81, 154.16, 141.54, 130.77, 120.07, 114.40, 56.12.

difluoro-boron complex of 2,2'-di-5-methoxyquinolyamine (2d): In a three-neck round bottom flask, the ligand, 2,2'-di-5-methoxyquinolyamine (2d₁) (500 mg, 1.51 mmol) was dissolved in dry toluene under N₂. DIEA (0.79 ml, 4.53 mmol) was slowly injected to the solution. After 30 min of stirring, BF₃OEt₂ (0.745 ml, 6.04 mmol) was slowly added dropwise to the solution. The reaction was then left to reflux overnight. After cooling to room temperature, saturated solution of NaHCO₃ aq was added to the reaction mixture, followed by extraction from CH₂Cl₂. The combined organic layers were dried over MgSO₄, and solvent removed under reduced pressure. The crude product was purified by silica gel chromatography (2% methanol/CH₂Cl₂) to afford a yellow solid. The desired product was further sublimed at 200 °C under 1.2 × 10⁻⁶ torr. ¹H NMR (400 MHz, CDCl₃) δ 8.07 (q, *J* = 2.7 Hz, 1H), 7.95 – 7.91 (m, 1H), 7.59 (d, *J* = 8.7 Hz, 1H), 7.10 – 7.01 (m, 2H), 4.02 (s, 3H). ¹³C NMR (101 MHz, DMSO-*d*₆) δ 161.81, 154.16, 141.54, 139.58, 130.77, 120.07, 114.40, 104.60, 56.12. Elemental Analysis: calc. (C, 63.35; H, 4.25; N, 11.08), found (C:59.38 H:4.46 N:10.12)

difluoro-boron complex of 2,2'-diisoquinolyamine (3): Synthesis of the ligand for **3** is similar to that of **2a**₁ but used 1-chloroisoquinoline instead of 2-chloroquinoline and 1-aminoisoquinoline for 2-aminoquinoline as precursors. Similar borylation condition to **2a** were conducted on the formed 2,2'-diisoquinolyamine ligand to form compound **3**. ¹H NMR (400 MHz, DMSO-*d*₆) δ 9.19 – 9.11 (m, 2H), 7.98 – 7.89 (m, 6H), 7.86 – 7.75 (m, 2H), 7.48 (dt, *J* = 7.0, 1.0 Hz, 2H). ¹³C NMR (101 MHz, dmsO) δ 152.56, 136.90, 134.04, 129.61, 129.03, 127.88, 127.12, 114.80. Elemental Analysis: calc. (C, 67.75; H, 3.79; N, 13.17), found (C, 67.11; H, 3.97; N, 12.50)



Scheme S6: Synthesis of **4**.

N-(isoquinolin-1-yl)-5-methoxyquinolin-2-amine (4'): bis(2-diphenylphosphinophenyl) ether (23.56 mg, 43.74 μmol), 2-amino-5-methoxyquinoline (200 mg, 1.15 mmol), 1-chloroisoquinoline (187.83 mg, 1.15 mmol) and t-BuONa (147.12 mg, 1.53 mmol), and Pd(OAc)₂ (9.82 mg, 43.74 μmol) catalyst were added to a three-neck round bottom flask. The air free flask and refluxed in a 110°C oil bath for

48 hours. The flask was subjected to three cycles of evacuation-backfilling with N₂. Dry toluene purged with N₂ was transferred to the reaction mixture using a cannula. The reaction was refluxed for 48 h at 110 °C under inert atmosphere. After that, the mixture was cooled to room temperature, extracted from CH₂Cl₂, dried over MgSO₄, and solvent removed under reduced pressure. The crude product was then purified using a silica gel column chromatography (2% methanol/CH₂Cl₂). ¹H NMR (400 MHz, CDCl₃) δ 8.71 (d, *J* = 5.5 Hz, 1H), 8.41 (ddt, *J* = 8.0, 1.4, 0.7 Hz, 1H), 8.01 – 7.45 (m, 7H), 7.14 (dd, *J* = 6.2, 0.9 Hz, 1H), 7.07 – 7.01 (m, 1H), 6.51 (d, *J* = 7.3 Hz, 1H), 3.59 (d, *J* = 3.6 Hz, 2H).

difluoro-boron complex of N-(isoquinolin-1-yl)-5-methoxyquinolin-2-amine (4): In a three-neck round bottom flask, the ligand, N-(isoquinolin-1-yl)-5-methoxyquinolin-2-amine (4') (300 mg, 1.0 mmol) was dissolved in dry toluene under N₂. DIEA (0.52 ml, 2.99 mmol) was slowly injected to the solution. After 30 min of stirring, BF₃OEt₂ (0.491 ml, 3.98 mmol) was slowly added dropwise to the solution. The reaction was then left to reflux overnight. After cooling to room temperature, saturated solution of NaHCO₃ aq was added to the reaction mixture, followed by extraction from CH₂Cl₂. The combined organic layers were dried over MgSO₄, and solvent removed under reduced pressure. The crude product was purified by silica gel chromatography (2% methanol/CH₂Cl₂) to afford a yellow solid. The desired product was further sublimed at 200 °C under 1.2 × 10⁻⁶ torr. ¹H NMR (400 MHz, CDCl₃) δ 9.00 (s, 1H), 8.01 – 7.89 (m, 3H), 7.83 – 7.76 (m, 1H), 7.74 – 7.63 (m, 2H), 7.60 (d, *J* = 8.7 Hz, 1H), 7.20 (t, *J* = 8.5 Hz, 2H), 7.07 (dd, *J* = 8.7, 2.4 Hz, 1H), 4.01 (s, 3H). ¹³C NMR (101 MHz, DMSO) δ 166.52, 159.29, 156.77, 154.35, 146.16, 141.46, 138.68, 135.43, 134.44, 133.57, 131.72, 125.48, 125.47, 119.67, 119.21, 119.19, 60.73. Elemental Analysis: calc. (C, 65.36; H, 4.04; N, 12.04), found (C, 65.23; H, 4.03; N, 11.66)

Photophysical Characterization

All samples in fluid solution were dissolved in 2-methyltetrahydrofuran with absorbance between 0.05-0.15 to prevent reabsorption when using the integrating sphere for Φ_{PL} measurements due to the small stoke-shift in the aD series. Doped poly(methylmethacrylate) thin films were prepared from a solution of poly(methylmethacrylate) (PMMA). 0.1 g of PMMA pellets were mixed with 1mL of dichloromethane. After all pellets have dissolved, 1 volume percent samples were made with **1**, **2** and **3**. 1 mg of chosen aD derivative was dissolved in the PMMA solution and 1mL was spin coated on a quartz substrate (2cm x 2 cm) using a pipet with the substrate rotating at 700 rpm for 45 seconds. The film was left to air dry. The UV-visible spectra were recorded on a Hewlett-Packard 4853 diode array spectrometer. Steady State fluorescence emission measurements were performed using a QuantaMaster Photon Technology International spectrofluorometer. Gated phosphorescence measurements were carried on the fluorimeter with 500 microsecond delay where the sample is in 77 K temperature. All reported spectra are corrected for photomultiplier response. Fluorescence lifetime measurements were performed using an IBH Fluorocube instrument equipped with 331 nm LED and 405 nm laser excitation sources using a time-correlated single photon counting method. Quantum yield values were obtained using a C9920 Hamamatsu integrating sphere system.

Table S1. Calculated and Experimental S1 and T1 energies for 1a-1b, 2a-2d, 3 and 4, where the difference between the two energies are represented by $\Delta E(S_1-T_1)$.

aD series	ϵ ($10^5 \text{ M}^{-1} \text{ cm}^{-1}$) ^a	Calculated results ^b			Experimental results ^c		
		S ₁ (eV/nm)	T ₁ (eV/nm)	$\Delta E(S_1-T_1)$	S ₁ (eV/nm)	T ₁ (eV/nm)	$\Delta E(S_1-T_1)$
1a	0.31	3.14/395	2.66/467	0.49	3.11/398	2.67/464	0.44
1b	-	2.85/436	2.51/495	0.34	3.02/409	2.68/463	0.34
2a	0.83	2.73/455	2.40/517	0.33	2.86/433	2.56/484	0.30
2b	0.96	2.65/469	2.35/529	0.30	2.81/440	2.51/494	0.30
2c	0.88	2.76/450	2.44/509	0.32	2.81/441	2.54/488	0.27
2d	1.30	2.79/444	2.48/500	0.31	2.80/442	2.50/496	0.30
3	0.50	2.78/447	2.41/515	0.37	2.93/422	2.49/498	0.44
4	0.78	2.78/447	2.43/510	0.35	2.86/433	2.47/502	0.39

a: Molar absorptivity values measured in tetrahydrofuran (THF)

b: TD-DFT B3LYP/6-311G** with 0.44 eV correction applied to the S₁ energies

c: Singlet energies are extrapolated from peak max of fluorescence (298 K) and triplet energies from gated phosphorescence (77 K) in 2-methyltetrahydrofuran (2-MeTHF)

Table S2. Summary of the photophysical parameters for 1a-1b, 2a-2d, 3 and 4.^a

	$\lambda_{\text{abs}}/\lambda_{\text{em max}}$ (nm) ^a	Φ_{PL} ^a	τ (ns) ^a	k_{r} 10^8 (s ⁻¹) ^b	k_{nr} 10^7 (s ⁻¹) ^c	$\lambda_{\text{em max}}$ (nm) ^d	Φ_{PL} ^d	τ (ns) ^d	k_{r} 10^8 (s ⁻¹) ^b	k_{nr} 10^7 (s ⁻¹) ^c
1a	398/404	0.42	2.1	2.0	27	402	0.48	2.34	2.05	22.2
1b	409/429	0.30	2.1	1.4	34	-	-	-	-	-
2a	433/434	0.86	3.3	2.7	4.3	432	0.86	3.37	2.55	4.15
2b	440/444	0.87	3.8	2.3	3.4	-	-	-	-	-
2c	441/442	0.84	3.3	2.6	4.9	-	-	-	-	-
2d	441/442	0.84	3.3	2.6	4.9	-	-	-	-	-
3	422/432	0.87	3.2	2.8	4.1	430	0.90	2.92	3.00	3.4
4	433/437	0.90	2.8	3.2	3.6	-	-	-	-	-

^a Recorded in 2-MeTHF. ^b $k_{\text{r}} = \Phi_{\text{PL}}/\tau$. ^c $k_{\text{nr}} = (1-\Phi_{\text{PL}})/\tau$. ^d Recorded in PMMA (1% doping)

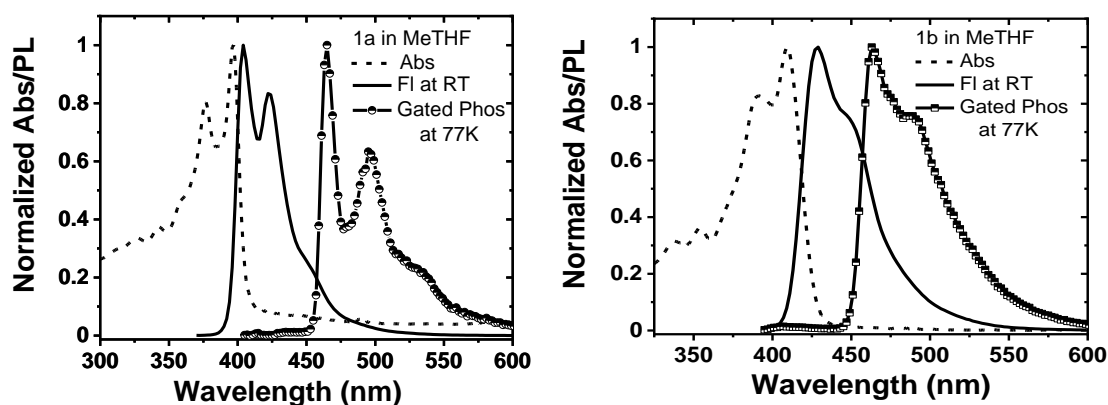


Figure S1. Normalized Spectra of absorbance (dash), fluorescence (solid) at 298K, and phosphorescence emission at 77K in 2-MeTHF for 1a and 1b

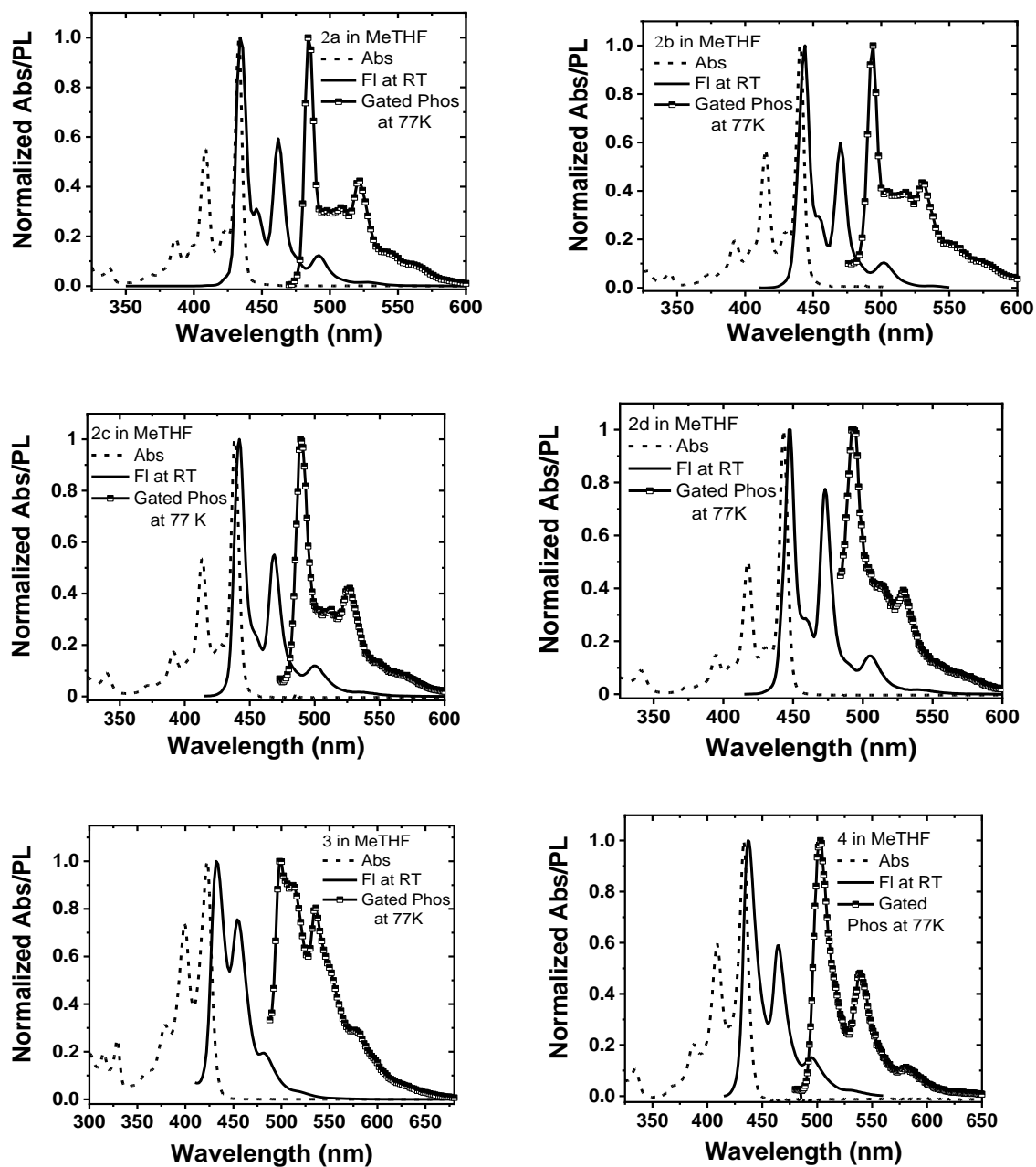


Figure S2. Normalized Spectra of absorbance (dash), fluorescence (solid) at 298K, and phosphorescence emission at 77K in 2-MeTHF for **2a**, **2b**, **2c**, **2d**, **3** and **4**.

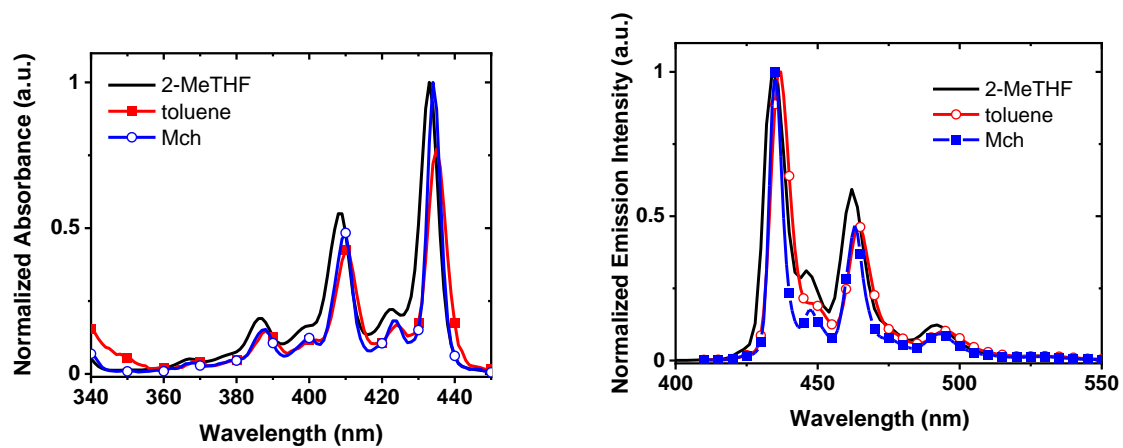


Figure S3. Normalized absorbance and emission of 2a in three different solvents; 2-methyltetrahydrofuran (2-MeTHF), toluene and methylcyclohexane (Mch).

Electrochemistry

Cyclic voltammetry and differential pulsed voltammetry were performed using a VersaSTAT potentiostat measured at 100 mV/s scan. Anhydrous acetonitrile (DriSolv) from Sigma Aldrich was used as the solvent under nitrogen environment, and 0.1 M tetra(n-butyl)ammoniumhexafluorophosphate (TBAF) was used as the supporting electrolyte. A glassy carbon rod was used as the working electrode; a platinum wire was used as the counter electrode, and a silver wire was used as a pseudoreference electrode. The redox potentials are based on values measured from differential pulsed voltammetry and are reported relative to a ferrocene/ferrocenium ($\text{Cp}_2\text{Fe}/\text{Cp}_2\text{Fe}^+$) redox couple used as an internal reference, while electrochemical reversibility was determined using cyclic voltammetry. **Table S3** tabulates the HOMO and LUMO energies extrapolated from calculations and the redox potentials in acetonitrile (ferrocene used as internal standard).

Table S3. HOMO and LUMO energies (in eV) for **1a-1b, 2a-2d, 3** and **4**.

	HOMO ^a	LUMO ^a	HOMO ^b	LUMO ^b
1a	-5.85	-2.12	-5.82	-1.85
1b	-5.62	-1.77	-5.52	-1.71
2a	-6.11	-2.58	-5.88	-2.34
2b	-6.03	-2.49	-5.71	-2.26
2c	-6.04	-2.39	-5.80	-2.23
2d	-5.87	-2.44	-5.71	-2.10
3	-6.06	-2.36	-5.82	-2.23
4	-5.99	-2.31	-5.74	-2.15

^a HOMO/LUMO energies extrapolated from experimental redox potentials. HOMO = 1.15 (E_{ox}) + 4.79; LUMO = 1.18 (E_{red}) - 4.83. ^b HOMO/LUMO values extrapolated from calculations (B3LYP/6-311G^{**}).

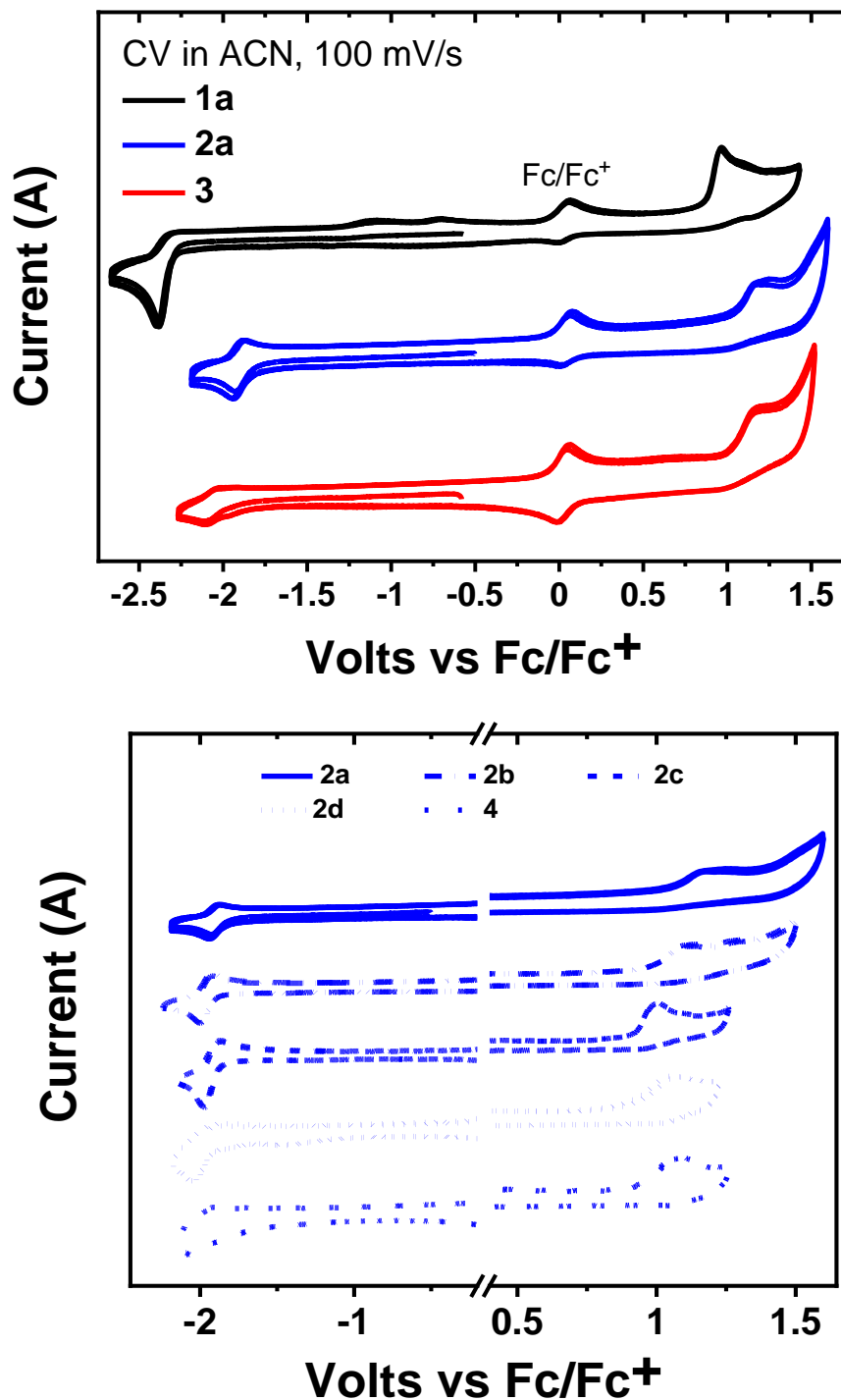


Figure S4. Cyclic Voltammetry for the compounds in acetonitrile vs ferrocene (100 mV/s).

TDDFT Calculations

All calculations reported in this work were performed using the Q-Chem 5.1 program². Ground-state optimization calculations were performed using the B3LYP functional and the 6-311G** basis set. Time dependent density functional theory (TDDFT) calculations were used to obtain the excitation energies and optimized geometries of the S₁ state at the same level. The S₁ energies were corrected by subtracting 0.44 eV to offset the large errors commonly associated with cyanine-like dyes.³

The extent of overlap (Λ) associated with the electronic transition from the ground state to the S₁ state was computed using the natural transition orbitals (NTOs) according to the following expression:

$$\Lambda = \frac{\sum_k \sigma_k \int |e_k \phi| |h_k \phi| d\tau}{\sum_k \sigma_k}$$

where, $e_k \phi$ and $h_k \phi$ are the electron and hole NTO pairs and σ_k is the amplitude of the corresponding NTO pair. The value of Λ would be bounded below by 0 for purely CT transitions with no spatial overlap and bounded above by ≈ 1 for strongly localized excitations. The computed Λ values and experimental S₁-T₁ gaps of the aD series were compared with those of anthracene⁴ and 4CzIPN⁵ and are shown in **Table S4**. The integrals are computed numerically for each NTO pair using the ORBKIT⁶ and Cubature⁷ python libraries. An in-house python code was used to compute Λ from the NTOs generated by Q-Chem in Molden format. The source code is available on GitHub (<https://github.com/danielsylvinson/OverlApp>) and the pre-built binaries (for Windows only) can be downloaded from SourceForge (<https://sourceforge.net/projects/overlapp>). The summary of the calculated excited state energies (in eV) at S₀ and S₁ optimized geometries (B3LYP/6-311G**) are tabulated in **Table S5**. The molecular orbital representation of compounds **1a-1b**, **2a-2d**, **3** and **4** at the B3LYP/6-311G** level optimized at S₀ geometry are shown in **Table S6**.

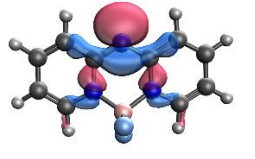
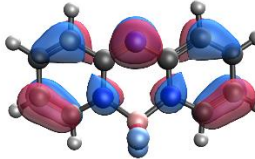
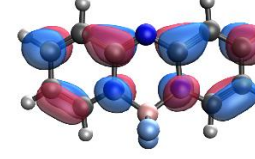
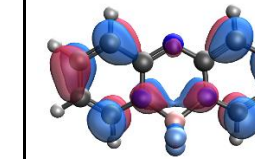
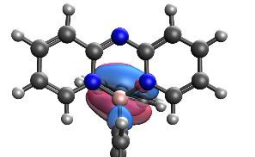
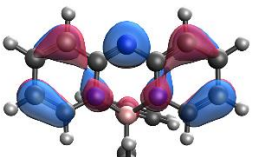
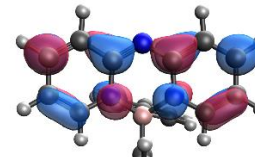
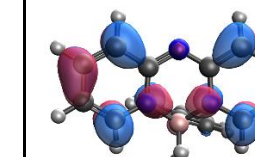
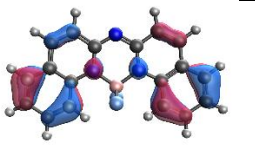
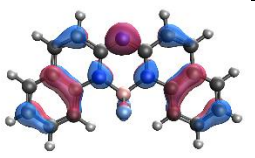
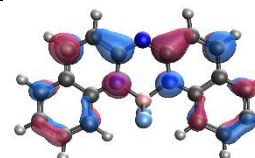
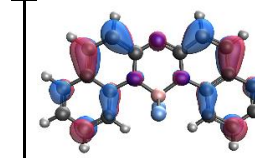
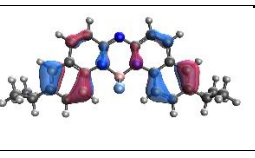
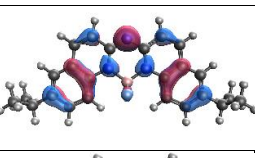
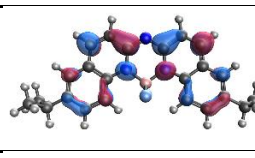
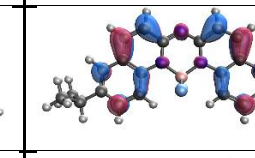
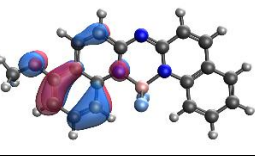
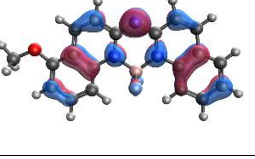
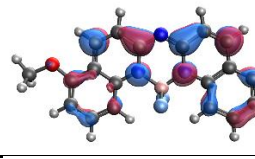
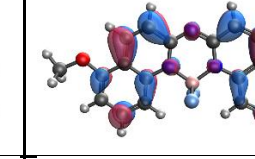
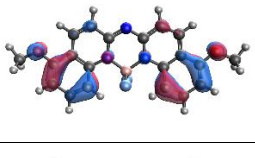
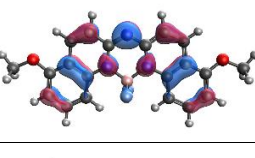
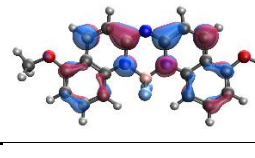
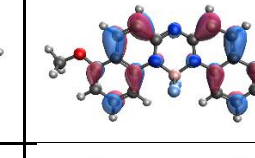
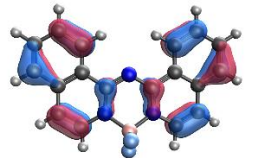
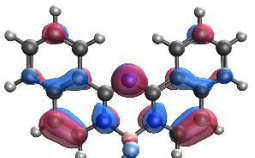
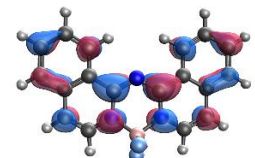
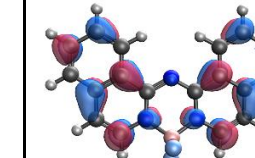
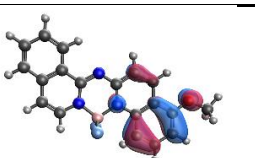
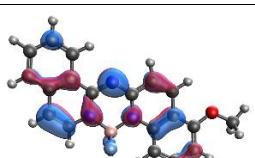
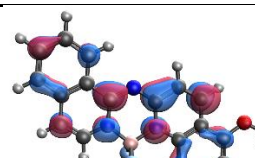
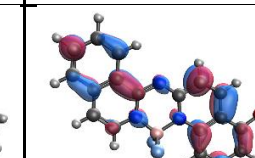
Table S4. Extent of overlap calculation using TDDFT with experimental comparison.

Compound	Λ	Exp S_1/T_1 energies (eV)	Exp S_1-T_1 gap
anthracene	0.84	3.10/1.78	1.32
1a	0.68	3.11/2.67	0.44
1b	0.65	3.02/2.68	0.34
2a	0.63	2.86/2.56	0.30
2b	0.61	2.81/2.56	0.30
2c	0.66	2.81/2.50	0.27
2d	0.66	2.80/2.51	0.30
3	0.66	2.93/2.49	0.44
4	0.68	2.86/2.47	0.39
4CzIPN	0.29	2.49/2.43	0.06

Table S5. Calculated excited state energies (in eV) at S_0 and S_1 optimized geometries. (B3LYP/6-311G**) for **2a-2d**, **3** and **4**.

Compound	S_1/T_2 energies		S_1-T_2	
	At S_0 geometry	At S_1 geometry	At S_0 geometry	At S_1 geometry
2a	2.73/2.92	2.40/2.71	-0.19	-0.31
2b	2.65/2.90	2.38/2.71	-0.26	-0.33
2c	2.76/2.79	2.41/2.71	-0.03	-0.30
2d	2.79/2.81	2.48/2.60	-0.01	-0.13
3	2.78/2.95	2.87/2.49	-0.18	-0.21
4	2.78/2.81	2.84/2.47	-0.03	-0.32

Table S6. Molecular orbital representation of compounds 1a-1b, 2a-2d, 3 and 4 at the B3LYP/6-311G** level.

	HOMO-1	HOMO	LUMO	LUMO+1
1a				
1b				
2a				
2b				
2c				
2d				
3				
4				

Organic LEDs

OLEDs were fabricated and tested by Glass substrates with pre-patterned, 1 mm wide indium tin oxide (ITO) stripes were cleaned by sequential sonication in tergitol, deionized water, acetone, and isopropanol, followed by 15 min UV ozone exposure. Organic materials and metals were deposited at rates of 0.5-2 Å/s through shadow masks in a vacuum thermal evaporator with a base pressure of 10⁻⁷ Torr. A separate shadow mask was used to deposit 1 mm wide stripes of 100 nm thick Al films perpendicular to the ITO stripes to form the cathode, resulting in 2 mm² device area. The device structure is: glass substrate/70 nm ITO/10 nm dipyrzino[2,3,-f:20,30-h]quinoxaline 2,3,6,7,10,11-hexacarbonitrile (HATCN)/45 nm 4,4'-cyclohexylidenebis [N,N-bis(4-methylphenyl)benzenamine] (TAPC)/1 vol% α -D: 4,4'-Bis(N-carbazolyl)-1,1'-biphenyl (CBP) host or 1 vol% α -D: N,N'-di(1-naphthyl)-N,N'-diphenyl-(1,1'-biphenyl)-4,4'-diamine (NPD)/45 nm 4,7-Diphenyl-1,10-phenanthroline (BPhen)/1.5 nm (8-Quinolinolato)lithium (LiQ) /100 nm Al. A semiconductor parameter analyzer (HP4156A) and a calibrated large area photodiode that collected all light exiting the glass substrate were used to measure the J-V-luminance characteristics. The device spectra were measured using a fiber-coupled spectrometer.

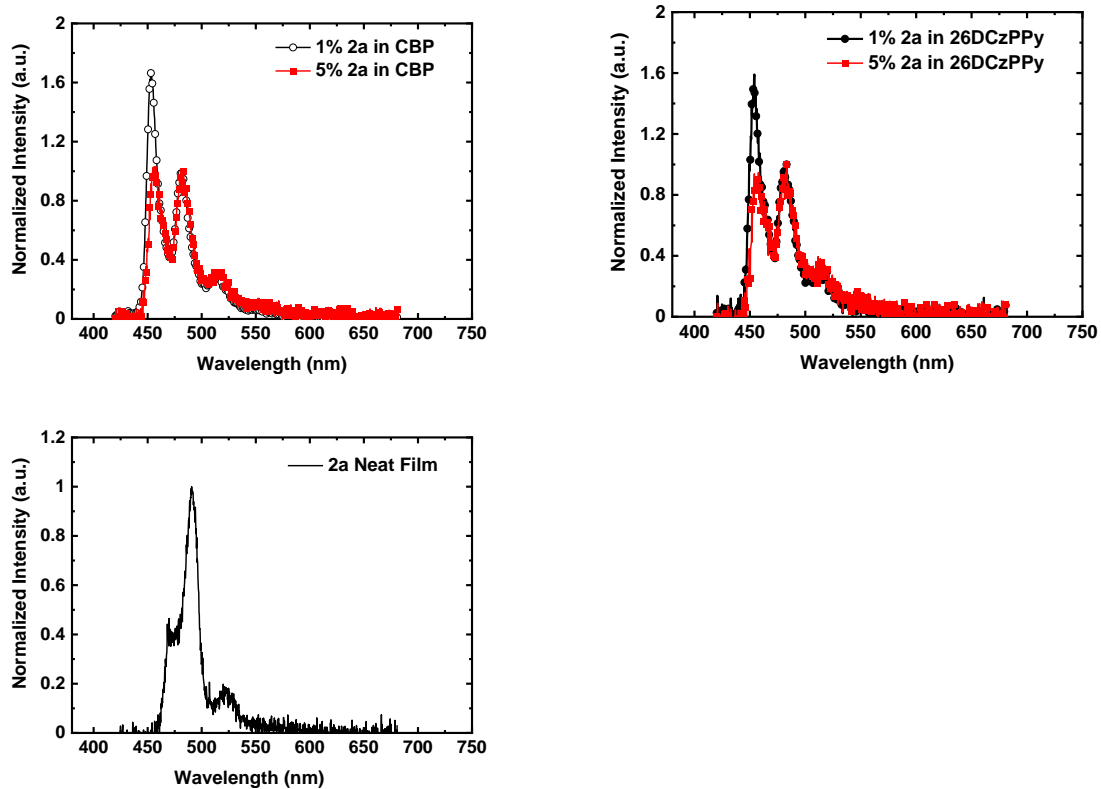


Figure S5. Photoluminescence data for doped and neat 2a films, which shows a decrease in the emission peak around 450 nm of **2a** due to reabsorption as concentration increases.

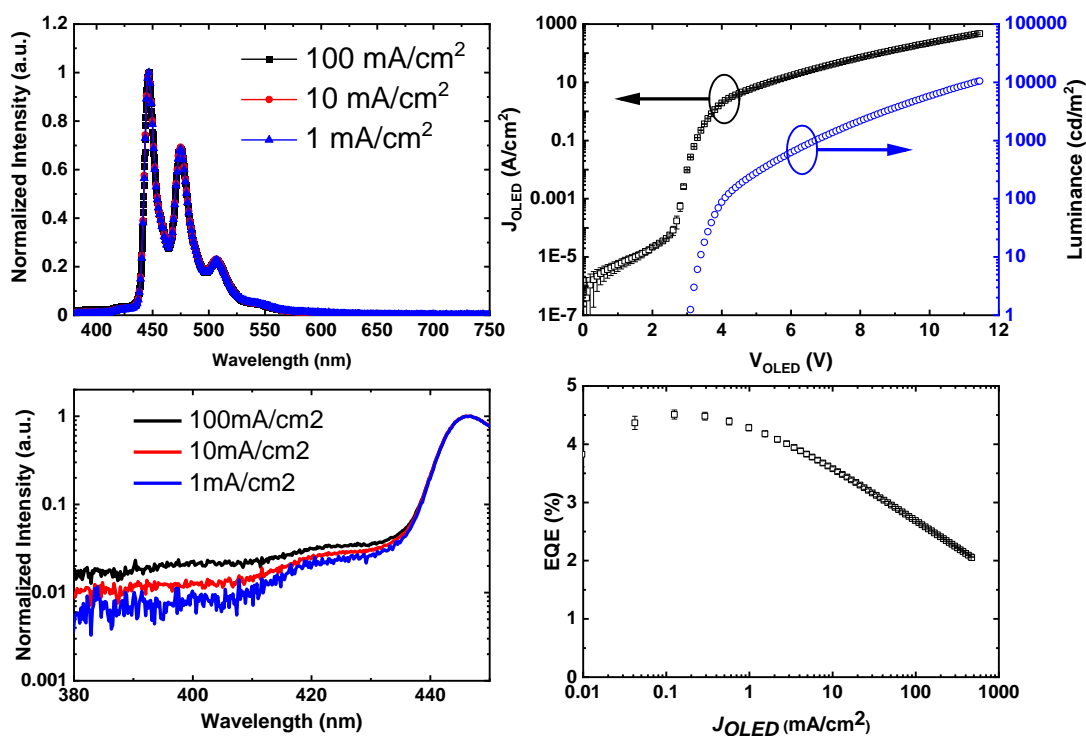


Figure S6. OLED data for 1% **2a** doped film with CBP as host. (top left) Electroluminescence vs. wavelength data illustrates that the electroluminescence emission is maintained with increasing current scans in the device (top right) The graph depicts the current vs. voltage and the luminance vs. voltage of the OLED. The device has a turn on voltage of 3 V. (bottom left) There is a small growing peak with increasing current which suggest charge leakage in the device (bottom right) EQE vs current data suggests that 1% **2a** doped film with CBP has an EQE_{max} of 4.5%.

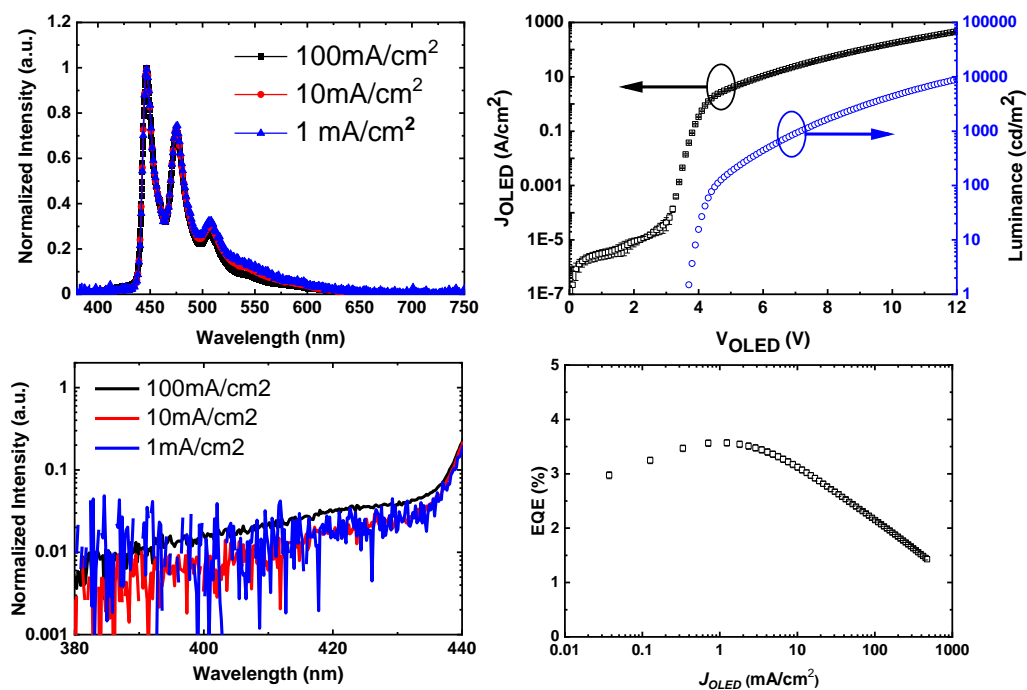


Figure S7. OLED data for 1% **2a** doped film with 26DCzPPY as host. (top left) Electroluminescence vs. wavelength data illustrates that the electroluminescence emission is maintained with increasing current scans in the device (top right) The graph depicts the current vs. voltage and the luminance vs. voltage of the OLED. The device has a turn on voltage of 3.7 V. (bottom left) There is a small growing peak with increasing current which suggest charge leakage in the device (bottom right) EQE vs current data suggests that 1% **2a** doped film with 26DCzPPY has an EQE_{max} of 3.5%.

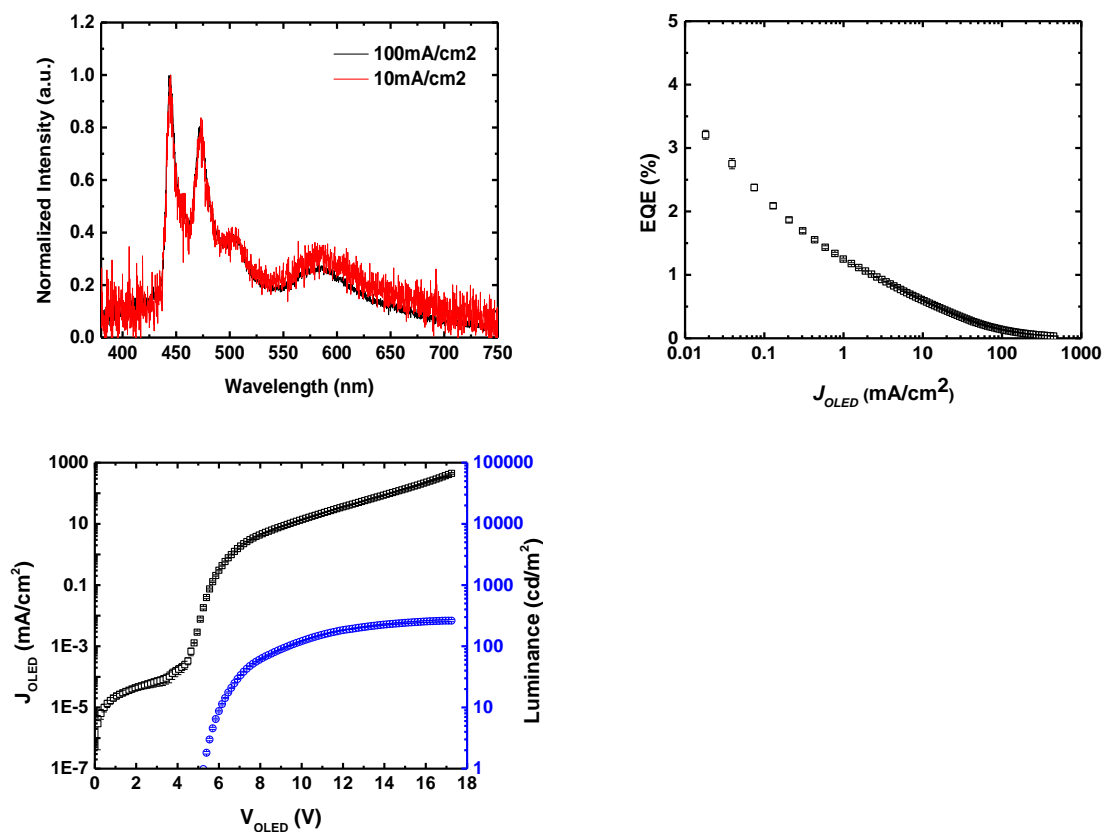


Figure S8. OLED data for 1% **2a** doped film with DPEPO as host. The device was fabricated using structure different to CBP and 26DCzPPy. ITO (70nm)/HATCN (10nm)/TAPC (40nm)/mCP(10nm)/DPEPO: 1% vol. **2a** (15nm)/ TSP01 (35nm)/TPBi (35nm)/ LiQ (1.5nm)/ Al (100nm). (top left) A broad exciplex emission is observed between 550 nm-750 nm. (top right) Rapid decline in the EQE with increasing current was observed. (bottom left) The DPEPO device is more resistive than CBP and 26DCzPPy with a turn-on voltage of 5 V.

Thermogravimetric Analysis of azaDIPYR, α -azaDIPYR and α -DIPYR

Thermal gravimetric analysis (TGA) was performed on a TGA Q50 instrument and samples were run in an alumina crucible under a flowing nitrogen atmosphere with a heating rate of 10 °C/min and the traces are shown in **Figure S9**. azaDIPYR (**1a**) sublimates cleanly and completely; the sublimation starts at *ca* 200°C and is complete by 280°C. α -azaDIPYR (**2a**) starts sublimation at a higher temperature \sim 275°C than azaDIPYR (**1a**) but has similar sublimation temperature range found in α -DIPYR. Benzannulation of the azaDIPYR (**1a**) core to α -azaDIPYR (**2a**) is enough to increase the sublimation properties by \sim 75°C. Purification of **2a** was carried out by sublimation at \sim 200 °C and 1.6×10^{-6} Torr. Decomposition were not observed during sublimation (for purification) or deposition of azaDIPYR materials for devices.

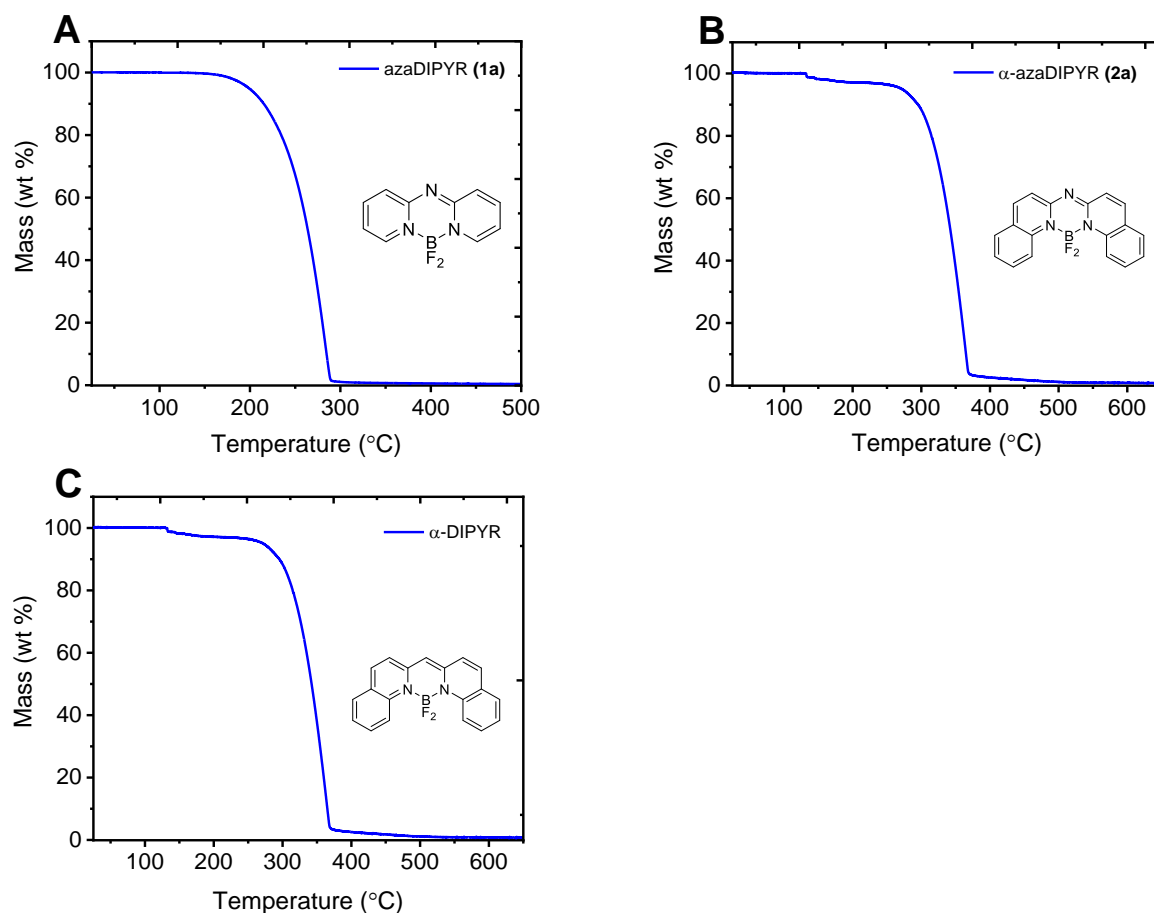


Figure S9. Thermogravimetric analysis curves for azaDIPYR (A), α -azaDIPYR (B), α -DIPYR³ (C).

References

1. (a) Wang, D.; Liu, R.; Chen, C.; Wang, S.; Chang, J.; Wu, C.; Zhu, H.; Waclawik, E. R., Synthesis, photophysical and electrochemical properties of aza-boron-diquinomethene complexes. *Dyes and Pigments* **2013**, *99* (1), 240-249; (b) Bañuelos, J.; Arbeloa, F. L.; Martínez, V.; Liras, M.; Costela, A.; Moreno, I. G.; Arbeloa, I. L., Difluoro-boron-triaza-anthracene: a laser dye in the blue region. Theoretical simulation of alternative difluoro-boron-diaza-aromatic systems. *Physical Chemistry Chemical Physics* **2011**, *13* (8), 3437-3445.
2. Shao, Y.; Gan, Z.; Epifanovsky, E.; Gilbert, A. T. B.; Wormit, M.; Kussmann, J.; Lange, A. W.; Behn, A.; Deng, J.; Feng, X.; Ghosh, D.; Goldey, M.; Horn, P. R.; Jacobson, L. D.; Kaliman, I.; Khaliullin, R. Z.; Kuś, T.; Landau, A.; Liu, J.; Proynov, E. I.; Rhee, Y. M.; Richard, R. M.; Rohrdanz, M. A.; Steele, R. P.; Sundstrom, E. J.; Woodcock, H. L.; Zimmerman, P. M.; Zuev, D.; Albrecht, B.; Alguire, E.; Austin, B.; Beran, G. J. O.; Bernard, Y. A.; Berquist, E.; Brandhorst, K.; Bravaya, K. B.; Brown, S. T.; Casanova, D.; Chang, C.-M.; Chen, Y.; Chien, S. H.; Closser, K. D.; Crittenden, D. L.; Diedenhofen, M.; DiStasio, R. A.; Do, H.; Dutoi, A. D.; Edgar, R. G.; Fatehi, S.; Fusti-Molnar, L.; Ghysels, A.; Golubeva-Zadorozhnaya, A.; Gomes, J.; Hanson-Heine, M. W. D.; Harbach, P. H. P.; Hauser, A. W.; Hohenstein, E. G.; Holden, Z. C.; Jagau, T.-C.; Ji, H.; Kaduk, B.; Khistyayev, K.; Kim, J.; Kim, J.; King, R. A.; Klunzinger, P.; Kosenkov, D.; Kowalczyk, T.; Krauter, C. M.; Lao, K. U.; Laurent, A. D.; Lawler, K. V.; Levchenko, S. V.; Lin, C. Y.; Liu, F.; Livshits, E.; Lochan, R. C.; Luenser, A.; Manohar, P.; Manzer, S. F.; Mao, S.-P.; Mardirossian, N.; Marenich, A. V.; Maurer, S. A.; Mayhall, N. J.; Neuscammann, E.; Oana, C. M.; Olivares-Amaya, R.; O'Neill, D. P.; Parkhill, J. A.; Perrine, T. M.; Peverati, R.; Prociuk, A.; Rehn, D. R.; Rosta, E.; Russ, N. J.; Sharada, S. M.; Sharma, S.; Small, D. W.; Sodt, A.; Stein, T.; Stück, D.; Su, Y.-C.; Thom, A. J. W.; Tsuchimochi, T.; Vanovschi, V.; Vogt, L.; Vydrov, O.; Wang, T.; Watson, M. A.; Wenzel, J.; White, A.; Williams, C. F.; Yang, J.; Yeganeh, S.; Yost, S. R.; You, Z.-Q.; Zhang, I. Y.; Zhang, X.; Zhao, Y.; Brooks, B. R.; Chan, G. K. L.; Chipman, D. M.; Cramer, C. J.; Goddard, W. A.; Gordon, M. S.; Hehre, W. J.; Klamt, A.; Schaefer, H. F.; Schmidt, M. W.; Sherrill, C. D.; Truhlar, D. G.; Warshel, A.; Xu, X.; Aspuru-Guzik, A.; Baer, R.; Bell, A. T.; Besley, N. A.; Chai, J.-D.; Dreuw, A.; Dunietz, B. D.; Furlani, T. R.; Gwaltney, S. R.; Hsu, C.-P.; Jung, Y.; Kong, J.; Lambrecht, D. S.; Liang, W.; Ochsenfeld, C.; Rassolov, V. A.; Slipchenko, L. V.; Subotnik, J. E.; Van Voorhis, T.; Herbert, J. M.; Krylov, A. I.; Gill, P. M. W.; Head-Gordon, M., Advances in molecular quantum chemistry contained in the Q-Chem 4 program package. *Molecular Physics* **2015**, *113* (2), 184-215.
3. Golden, J. H.; Facendola, J. W.; Sylvinson, M. R. D.; Baez, C. Q.; Djurovich, P. I.; Thompson, M. E., Boron Dipyridylmethene (DIPYR) Dyes: Shedding Light on Pyridine-Based Chromophores. *The Journal of organic chemistry* **2017**, *82* (14), 7215-7222.
4. Schols, S.; Kadashchuk, A.; Heremans, P.; Helfer, A.; Scherf, U., Triplet excitation scavenging as method to control the triplet concentration. *Proceedings of SPIE - The International Society for Optical Engineering* **2009**, 7415.
5. (a) Nakanotani, H.; Masui, K.; Nishide, J.; Shibata, T.; Adachi, C., Promising operational stability of high-efficiency organic light-emitting diodes based on thermally activated delayed fluorescence. *Scientific reports* **2013**, *3*, 2127-2127; (b) Cho, Y. R.; Cha, S. J.; Suh, M. C., Ideal combination of the host and dopant materials showing thermally activated delayed fluorescent behavior. *Synthetic Metals* **2015**, *209*, 47-54.
6. Hermann, G.; Pohl, V.; Tremblay, J. C.; Paulus, B.; Hege, H.-C.; Schild, A., ORBKIT: A modular python toolbox for cross-platform postprocessing of quantum chemical wavefunction data. *Journal of Computational Chemistry* **2016**, *37* (16), 1511-1520.
7. Castro, S. G. P.; Loukianov, A.; scku208; Dewing, M.; Bernardo Oliveira, J.; Arnold, D.; Eljarrat, A. *Python wrapper for Cubature: adaptive multidimensional integration*, v0.14.5; Zenodo: 2020.